第 51 卷 第 12 期/2024 年 6 月/中国激光 研究论文

中国激光

Q235钢扫描激光热丝焊接工艺特性与组织性能研究

于宸乾[1]，任刚[2]，黄映杰[2]，高明[1*]

[1]华中科技大学武汉光电国家研究中心，湖北 武汉 430074；

[2]九江中科激光技术研究院，江西 九江 332005

摘要 以Q235低碳钢为材料，研究了光束扫描对激光热丝焊的焊缝成形特性、微观组织和力学性能的影响。结果表明：在扫描激光的作用下，焊缝的成形变得更加均匀，飞溅减少，焊缝熔深减小，熔宽增大，截面熔合区底部变得更加平滑；扫描激光的加入降低了熔池的温度梯度，抑制了粗大柱状晶的生长，改变了铁素体晶粒形态，细化了熔合区组织，提高了焊缝韧性及延伸率；扫描激光促进了焊缝成分的均匀化分布，抑制了偏析，降低了熔合区显微硬度。由于激光作用面积增大等因素，光束扫描增强了激光热丝焊接对间隙的桥接能力。

关键词 激光技术；激光热丝焊接；光束扫描；微观组织；力学性能

中图分类号 TG456.7 **文献标志码** A **DOI**：10.3788/CJL230893

1 引 言

激光焊接具有热变形小、自动化程度高、加工效率高等优点，在汽车、船舶、微电子等领域中有着广泛的应用[1-3]。传统激光自熔焊接利用激光加热熔化基材以实现连接，由于聚焦光斑小（直径通常小于0.25 mm），其对焊件装配间隙的要求非常高。此外，高能激光束也会导致合金元素的蒸发烧损，并产生咬边、气孔和裂纹等缺陷，从而影响力学性能[4]。为了解决这些问题，研究者提出了激光填丝焊接技术。它不仅降低了对焊件的装配精度要求，而且通过填充材料，优化焊缝组织成分，提高力学性能。余阳春[5]采用激光填丝焊工艺焊接2.0 mm厚的铝合金板，即使间隙增至1.0 mm，焊缝仍成形良好、无塌陷。Li等[6]通过在7075高强铝合金的激光热丝焊中添加Sc粉，降低了焊缝气孔率，提高了接头的显微硬度、抗拉强度和伸长率。方乃文等[7]对比研究了TC3实心焊丝和Ti-Al-V-Mo药芯焊丝对TC4钛合金激光填丝焊接组织性能的影响，结果显示，与实心焊丝相比，药芯焊丝添加的元素没有导致焊缝偏析，焊缝组织晶粒更加细小，位错密度更高，焊接接头的抗拉强度、断后伸长率和显微硬度均较高。

在通常情况下，激光填丝焊接使用常温焊丝，也称激光冷丝焊。焊接时部分激光能量用于熔化焊丝，为了对熔池进行能量补偿，需要降低焊接速度[8]，这在一定程度上牺牲了效率优势。因此，研究者利用电流对焊丝进行提前预热，即激光热丝焊。对焊丝进行预热不仅可以增大焊丝对激光的吸收率，而且焊丝预热后熔化所需的激光能量大大减少，提高了填充效率[9]。Marumoto等[10]采用激光热丝焊接技术在5.7 m/min的高焊接速度下，获得了具有足够熔深且没有成形缺陷的JIS500钢板角焊缝。Wei等[11]针对FV520马氏体时效钢激光热丝堆焊建立了一个全面的多相模型，模型预测的焊缝形貌和实际焊接结果吻合良好，并分析了焊接过程中的马兰戈尼流动行为和温度场演变规律。Liu等[12]采用有限元方法分析了激光热丝焊接温度场对热致残余应力的影响，结果表明，当热丝电压降低时，残余应力特别是横向残余应力明显减小。郑世卿等[13]通过数学推导给出了激光热丝焊接中送入熔池的焊丝的温度表达式，并通过计算和高速摄影方法发现，当送入焊丝温度接近焊丝熔点时，焊丝的熔化过渡行为最稳定。然而，激光热丝焊接对焊丝尖端和激光焦点位置的对中精度要求较高，存在焊道弯曲和焊缝高度不均匀等问题[14]。因此，研究者又引入了激光束振荡扫描热丝焊接，降低了系统对光丝对中位置的要求，利用激光束高频扫描搅拌熔池，改变了熔池的温度梯度和凝固结晶过程，进而改善了焊缝表面成形以及微观组织结构[15]。Wu等[16]对比研究了不同类型的扫描模式对HLSA钢激光焊接成形和气孔的影响，发现圆形扫描时焊缝气孔率最低，能量分布更加均匀，最大功率密度仅为无扫描时的13%。陈根余等[17]采用扫描激光填丝焊接技术对2 mm厚的2060铝锂合金进行了实验研究，实验结果表明，焊接过程稳定，焊缝气孔得到有效抑制。

收稿日期：2023-06-06；**修回日期**：2023-06-27；**录用日期**：2023-08-01；**网络首发日期**：2023-08-15

基金项目：国家自然科学基金（52275335）、江西省重点研发计划（20212BBE51011）、中国博士后科学基金（2023M731173）

通信作者：*mgao@mail.hust.edu.cn

Li等[18]采用振荡激光热丝焊接的方法对20 mm厚的316L不锈钢进行了垂直焊接实验，结果表明，光束振荡促进了焊缝金属的润湿行为，减少了垂直焊接过程中的气孔缺陷。但是，目前关于扫描激光对焊缝显微组织和性能的影响研究还极其有限，尚无法为工业应用提供理论支撑。

本文以工业中常用的Q235低碳钢为研究对象，开展了扫描激光热丝焊接工艺研究。通过与常规激光热丝焊进行对比，研究了扫描参数对焊缝成形、缺陷和组织性能的影响，获取了扫描激光热丝焊接的优化工艺参数窗口，明晰了扫描激光对焊缝金属凝固过程的影响机制，为激光焊接应用范围的扩展提供了指导。

2 实验材料、设备及方法

2.1 实验材料

实验所用的基材为Q235碳素结构钢，其中，平板堆焊基板的厚度为3.5 mm，间隙对接基板的尺寸为50 mm×120 mm×2 mm。填充材料选用直径为1.0 mm的50C6实芯焊丝。基材和焊丝的化学成分如表1所示。

表1 基材和焊丝的化学成分(质量分数，%)

Table 1 Chemical compositions of base metal and welding wire (mass fraction, %)

Material	C	Si	Mn	P	S	Cu	Fe
Q235	0.180	0.300	0.450	0.045	0.050	–	Bal.
50C6	0.080	0.920	1.520	0.020	0.015	0.200	Bal.

2.2 实验装置及方法

如图1所示，本文采用的扫描激光热丝焊接实验平台主要包括光纤激光器、电弧焊机、工业机器人以及扫描振镜等。

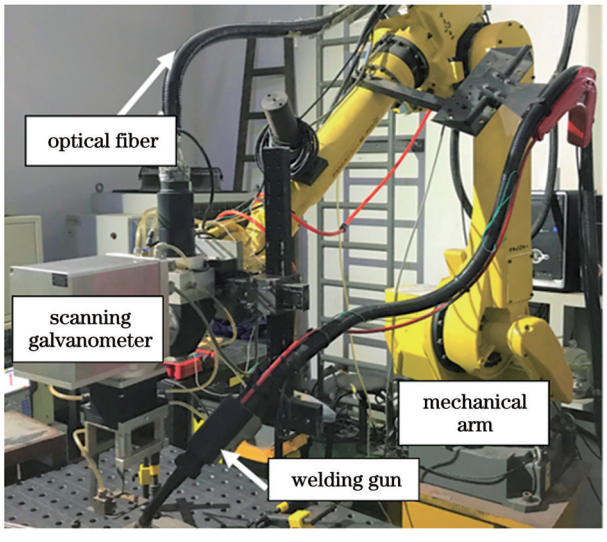

图1 扫描激光热丝焊接装置

Fig. 1 Oscillating laser hot wire welding device

优化的工艺布置和实验方法如图2所示，固定送丝方式为前置送丝，焊枪倾斜角度为45°，送丝落点与聚焦光斑重合，即激光一半作用于母材，一半作用于焊丝，这样布置是为了保证焊丝过渡模式是对熔池干扰程度较小的液桥过渡模式[19]。激光焦点位于被焊件表面，扫描图形为圆形，扫描振幅(A)等于圆的直径。焊接过程中保护气体为纯度(体积分数)大于99.99%的氩气，采用旁轴吹气方式，气管角度为60°，气体流量约为20 L/min。在激光填丝对接焊实验中，由于熔透状态下激光匙孔的动态稳定性更强，焊接产生的飞溅更少，焊缝组织更加均匀[20]，故本实验中所有对接焊均为全熔透状态。具体焊接参数如表2所示。

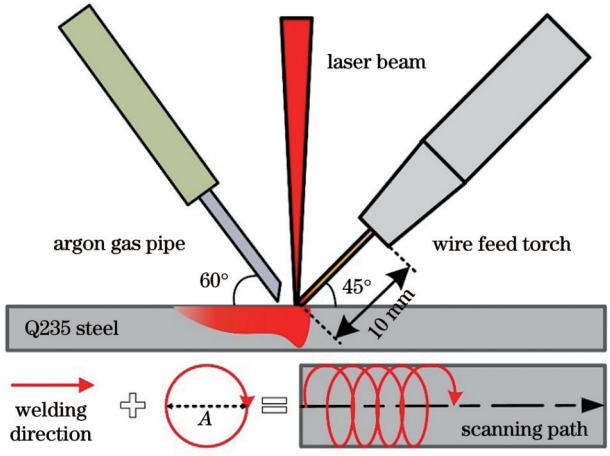

图2 扫描激光热丝焊接示意图

Fig. 2 Schematic of scanning laser hot wire welding

2.3 焊接接头组织分析

采用线切割机截取不同参数下的中部焊缝横截面，经过镶样、磨样、抛光后，使用质量分数为4%的硝酸乙醇对样品进行腐蚀，腐蚀时间为6～8 s。将样品烘干后使用扫描电镜(SEM)对金相样品进行观察，并使用其自带的能谱仪对焊缝组织进行元素分析。

2.4 焊接接头力学性能测试

采用硬度计对焊缝横截面进行硬度测试，测量位置位于焊缝横截面中心线及距离中心线上下0.2 mm的位置，如图3所示，测点间距为0.2 mm，实验加载力为9.8 N，保荷时间为20 s，结果取同一竖直线上三个点硬度的平均值。设计并切取拉伸样，如图4所示，使用拉伸试验机进行拉伸测试，拉伸速度为2 mm/min，结果取三个拉伸样的平均值。拉伸后同样使用扫描电镜观察断口。

3 实验结果与讨论

3.1 焊缝宏观形貌

如图5所示，扫描振幅和扫描频率对焊缝表面与截面形貌有着显著影响。当不加扫描激光时，焊缝正面存在局部不均匀现象，焊缝周围存在明显的飞溅带，飞溅颗粒较小但数量较多，焊缝截面底部尖锐，呈现明

表 2 焊接实验参数

Table 2 Experimental parameters for welding

Laser power P /kW	Welding speed V_w /(m/min)	Wire feed speed V_f /(m/min)	Hot wire current I /A	Scanning frequency f /Hz	Scanning amplitude A /mm	Clearance distance D /mm
1.8	1.0	1.5	0			0
1.8	1.0	1.5	100			0
1.8	1.0	1.5	100	100	0.6	0
1.8	1.0	1.5	100	200	0.6	0
1.8	1.0	1.5	100	100	0.8	0
1.8	1.0	1.5	100	200	0.8	0
1.8	1.0	1.5	100	100	1.0	0
1.8	1.0	1.5	100	200	1.0	0
1.8	1.0	3.0	0	0	0	0.6
1.8	1.0	3.0	0	0	0	0.8
1.8	1.0	3.0	0	0	0	1.0
1.8	1.0	3.0	0	0	0	1.1
1.8	1.0	3.0	100	0	0	1.1
1.8	1.0	3.0	100	0	0	1.2
1.8	1.0	3.0	100	50	1.0	1.2
1.8	1.0	3.0	100	50	1.0	1.3

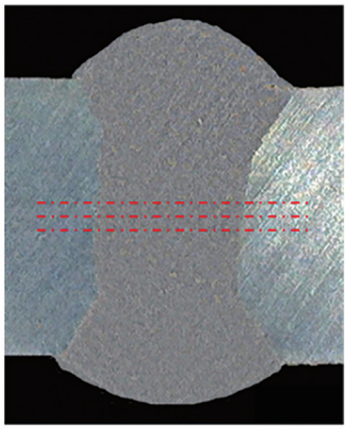

图 3 硬度测试位置

Fig. 3 Hardness test positions

显的钉子形。对比图 5(a)和图 5(b)可知，在引入扫描振幅 A=0.6 mm、扫描频率 f=100 Hz 的扫描激光束后，焊缝表面的飞溅明显减少，焊缝变得光滑平直。通过测量发现，焊缝熔深由无激光扫描时的 3.370 mm 下降到激光扫描时的 2.212 mm，下降了约 34%，焊缝熔宽由无激光扫描时的 2.037 mm 增大到激光扫描时的 2.327 mm，增大了约 14%，焊缝截面形状也由无激光扫描时的钉子形转变为激光扫描时的“U”形。显然，扫描激光的加入能使焊缝成形更加均匀，飞溅更少，说明扫描激光的加入能提高熔滴过渡的稳定性。

保持扫描振幅 A=0.6 mm 不变，增大扫描频率，对比图 5(b)和图 5(c)可以看出，当扫描频率为 100 Hz 时焊缝存在极少量的小颗粒飞溅，而当扫描频率为

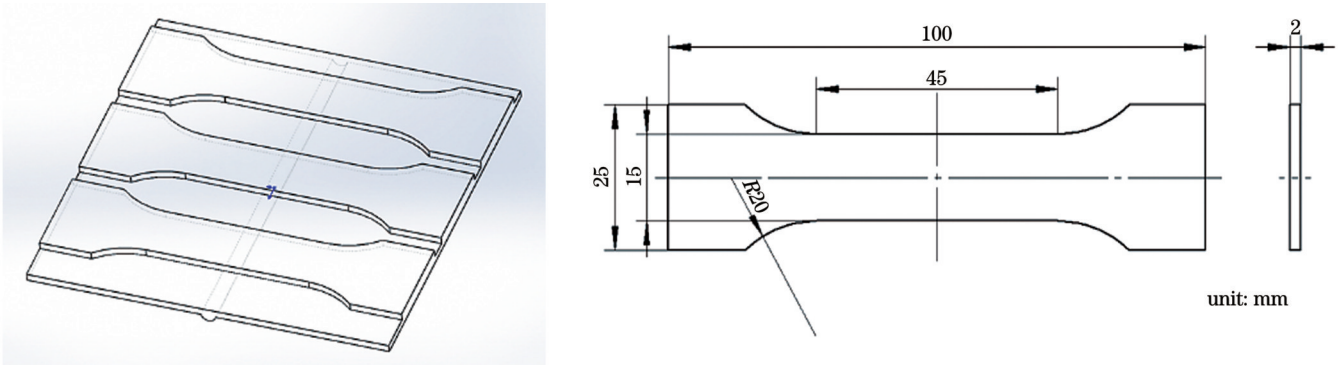

图 4 拉伸试样示意图。(a)取样示意图；(b)拉伸试样尺寸示意图

Fig. 4 Schematics of tensile specimen. (a) Sampling diagram; (b) diagram of tensile specimen size

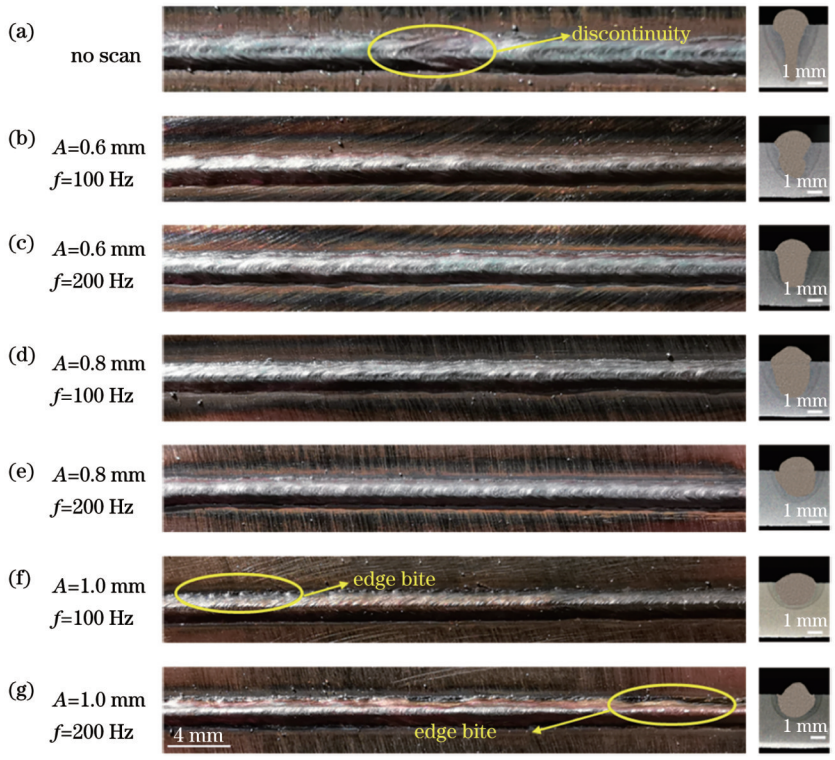

图 5　不同扫描参数下的焊缝表面与截面形貌

Fig. 5　Weld surface and cross section morphologies under different scanning parameters

200 Hz时，焊缝基本没有飞溅的产生。当扫描振幅增大到 1 mm时，焊缝表面出现咬边缺陷，如图 5(f)、(g)所示。当扫描频率从 100 Hz增大至 200 Hz时，咬边现象变得更加严重。这是因为当扫描频率增大到 100 Hz以上时，扫描激光束的能量分布特征为两侧能量高、中心能量低[21]，焊缝两侧的母材金属熔化较多，没有足够的熔融金属及时填充，因此出现了咬边现象。

3.2　微观组织分析

图 6所示为母材的微观组织，可以看出Q235钢的母材主要由铁素体组织构成。图 7(a)和图 7(b)分别为加入扫描激光前后焊缝中心的微观组织图片。对比可以发现：加入扫描激光前焊缝熔合区中心部位的组织含有粗大的柱状枝晶，主要由侧板条铁素体(FSP)和针状铁素体(AF)组成。这是因为加入扫描激光前

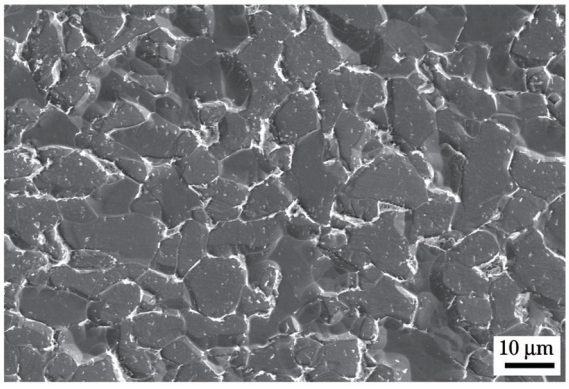

图 6　母材的微观组织

Fig. 6　Microstructure of base metal

焊缝中心的能量密度大，温度较高，有利于FSP在奥氏体晶界处形成，并快速生长，当其遇到新的铁素体

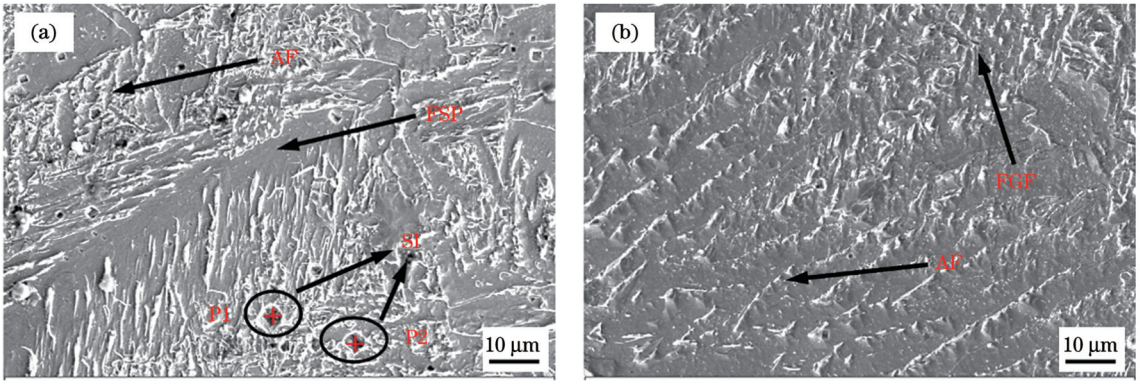

图 7　焊缝中心的微观组织。(a)加入扫描激光前；(b)加入扫描激光后

Fig. 7　Microstructures of weld centers. (a) Before adding scanning laser; (b) after adding scanning laser

(即针状铁素体)形核时,生长便受到阻碍[22]。加入扫描激光后焊缝熔合区中心部位主要为块状组织,由细晶铁素体(FGF)、针状铁素体等组织组成。熔合区的组织类型发生改变的原因是扫描激光焊接扩大了激光的作用范围,使熔池的能量分布更加均匀,降低了熔池的温度梯度,在散热条件不变的情况下,焊缝发生固态转变的温度较低,最终导致焊缝中心区域的组织以转变温度较低的细晶铁素体和针状铁素体为主。从图 7(a)还可以看出,加入扫描激光前在焊缝熔合区中存在固体夹杂(SI),这种硬脆相能增加焊缝的硬度,但其对焊接接头的韧性不利。为了进一步确定夹杂的具体成分,采用能谱仪(EDS)对夹杂成分进行测试,如图 7(a)所示,测点分别为 P1、P2。测试结果如图 8 所示,可以看出,P1 点和 P2 点处的成分均以 Fe 元素和 C 元素为主,含有微量的 Mn 元素和 Si 元素,未检测到氧元素,因此可以基本确定此处的夹杂成分为碳化铁。

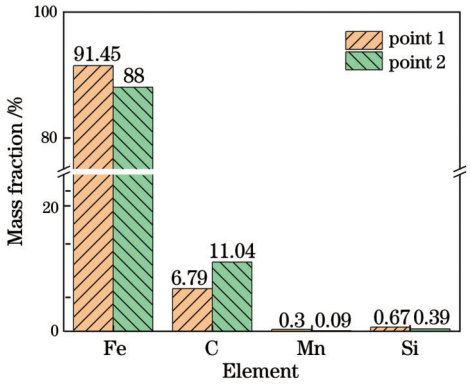

图 8　测点处元素的质量分数

Fig. 8　Mass fractions of elements at measuring points

图 9(a)、(b)分别为扫描激光热丝焊热影响区的粗晶区和细晶区的微观组织图片。由于激光和电流两种热源的共同作用,焊接热输入较大,粗晶区奥氏体晶粒的长大倾向严重,故冷却到室温时生成了上贝氏体(B_u)和粒状贝氏体(B_g)。细晶区距离熔合区更远,热输入较小,虽然原有的铁素体全部转化为奥氏体,但在凝固过程中奥氏体晶粒来不及长大,因此冷却到室温时奥氏体转变为大小不均的块状铁素体和珠光体(P)。

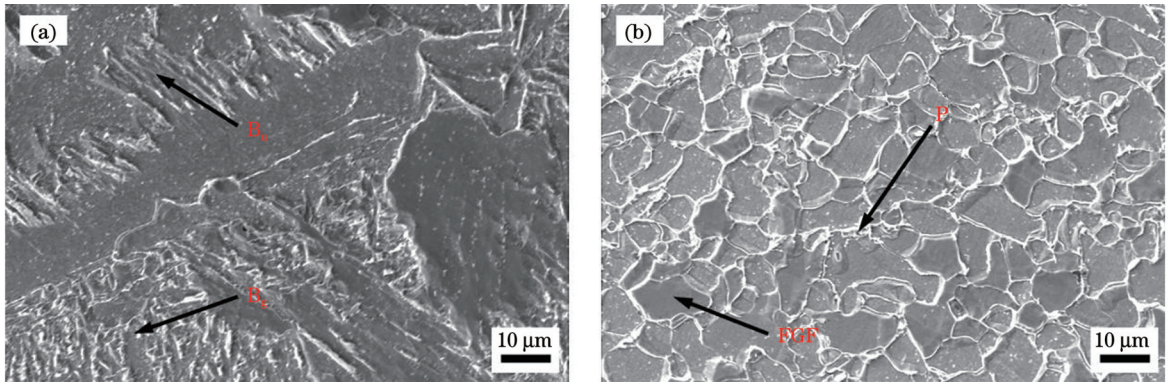

图 9　扫描激光热丝焊接热影响区的微观组织。(a)粗晶区;(b)细晶区

Fig. 9　Microstructure of heat affected zone in scanning laser hot wire welding. (a) Coarse-grained region ;(b) fine crystal region

3.3　焊接接头的力学性能及分析

3.3.1　拉伸性能

焊接接头的拉伸实验结果如表 3 所示,三种焊接工艺下的拉伸试样均断裂在焊缝熔合区(FZ)。激光热丝焊接接头的抗拉强度均值为 574.7 MPa,扫描激光热丝焊接接头的抗拉强度均值为 578.8 MPa,两者的抗拉强度基本相当,均优于激光冷丝焊接接头的抗拉强度(528.3 MPa)。但激光热丝焊接接头的拉伸断口延伸率为 8.4%,加入扫描激光后延伸率提高到 13.1%,提升了 55.9%。这是因为当扫描激光束在熔池内以一定的速度和轨迹移动时,熔池中产生了大量湍流,这些湍流不断冲击树枝晶的尖端,致使其断裂破碎,从而抑制了柱状枝晶的进一步生长[23]。这些破碎的晶粒被带入熔池并保存下来,成为了新晶粒形成时的晶核,提高了形核率,有利于焊缝晶粒的细化和等轴晶的形成,因此焊缝的韧性增强,接头延伸率提高。

表 3　不同焊接方法得到的焊接接头的拉伸实验结果

Table 3　Tensile test results of welded joints obtained by different welding methods

Welding method	Tensile strength /MPa	Elongation /%	Fracture position
Laser cold wire welding	528.3	5.8%	FZ
Laser hot wire welding	574.7	8.4%	FZ
Scanning laser hot wire welding	578.8	13.1%	FZ

图 10(a)、(b)、(c)分别为激光冷丝、激光热丝和扫描激光热丝焊接接头的拉伸断口形貌，可以看出，三种焊接方式得到的焊接接头的拉伸断口表面均覆盖着大量韧窝，表明三者均为典型的韧性断裂。其中激光冷丝焊接接头和激光热丝焊接接头的断口由尺寸较大的韧窝和其周围的小韧窝组成，而扫描激光热丝焊接接头的断口表现为较为均匀的等轴韧窝，因此其延伸率更大，韧性更好。从图 10 还可以看出，激光冷丝焊接接头和激光热丝焊接接头的断口韧窝底部均存在夹杂物，而扫描激光热丝焊接接头的断口韧窝底部没有发现夹杂物，说明扫描激光提高了焊缝成分的均匀性，抑制了偏析。

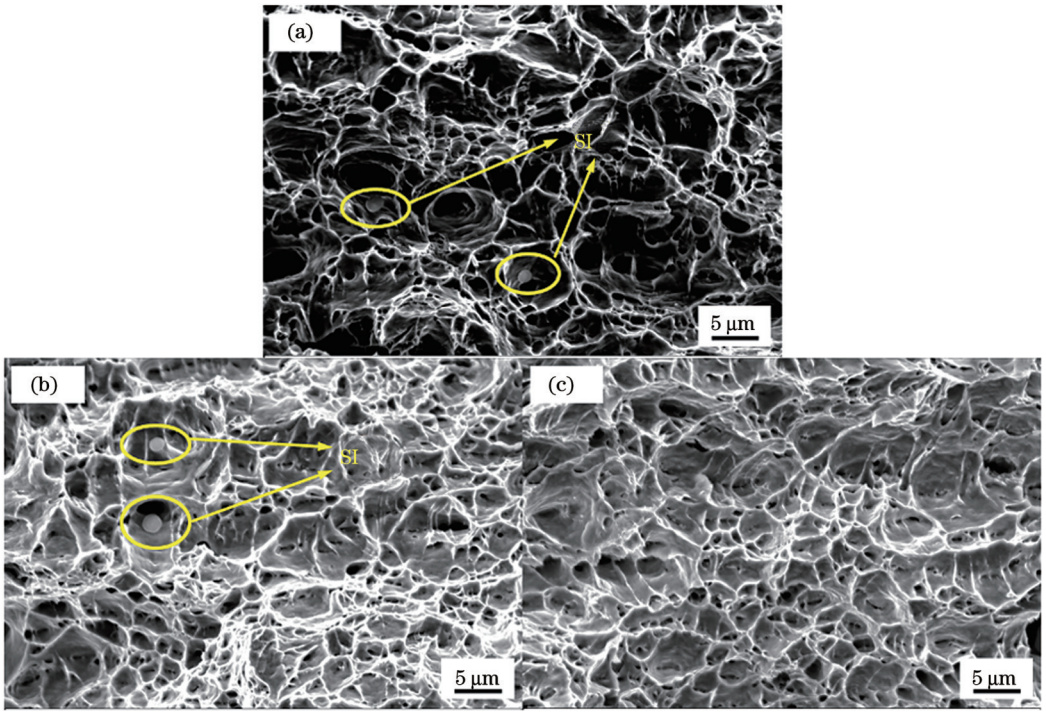

图 10　拉伸试样的断口形貌。(a)激光冷丝焊接接头；(b)激光热丝焊接接头；(c)扫描激光热丝焊接接头

Fig. 10　Fracture morphologies of tensile specimens. (a) Laser cold wire welded joints; (b) laser hot wire welded joints; (c) scanning laser hot wire welded joints

3.3.2　接头显微硬度

图 11(a)、(b)分别为加入扫描激光前后焊接接头的硬度分布。可以看出，两种焊接方式下焊接接头都是熔化区硬度最高，且热影响区(HAZ)的硬度高于母材(BM)但明显低于熔合区，这是因为两种焊接方式下焊接接头的熔合区均包含长短不一的针状和条状铁素体，其硬度大，韧性差。其中，加入扫描激光前焊缝熔合区的平均硬度为 197.8 HV，加入扫描激光后焊缝熔合区的平均硬度为 171.6 HV，后者相较于前者下降了约 13%。在扫描激光热丝焊接过程中，扫描激光束驱动的熔池强制流动占主导，且其显著强于激光热丝焊接过程中由表面张力差引起的 Marangoni 对流[24]，因此光束搅拌效应促进了液态金属完全凝固前的对流传质，有利于焊缝中溶质的均匀分布。而激光热丝焊

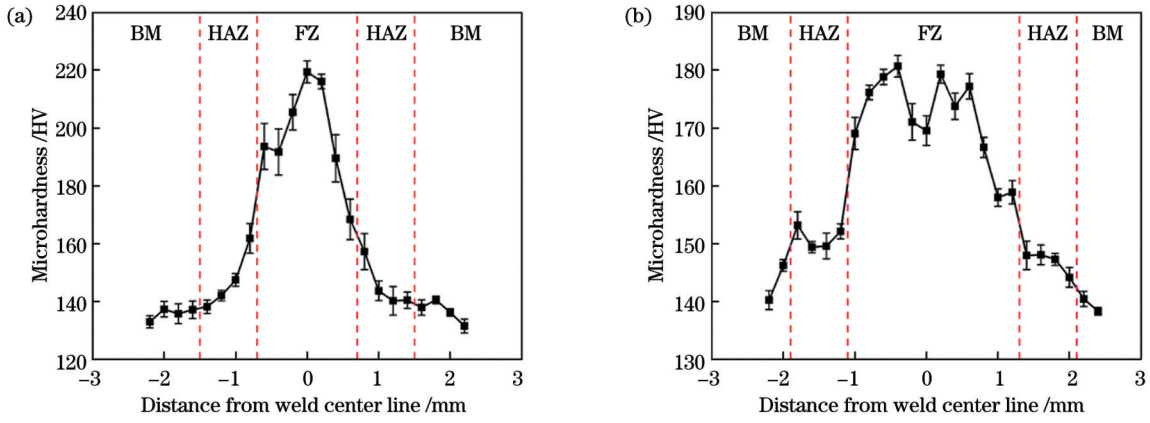

图 11　焊接接头的硬度分布。(a)激光热丝焊接；(b)扫描激光热丝焊接

Fig. 11　Hardness distributions of welded joints. (a) Laser hot wire welding; (b) scanning laser hot wire welding

接焊缝中心部位的激光能量集中，熔池的温度梯度大，成分过冷难以形成，柱状晶从熔合线向焊缝中心生长，将杂质“推”向熔池中心，从而造成区域偏析，在熔合区中形成了硬而脆的碳化物，提高了熔合区的显微硬度，但是降低了焊缝接头的韧性。

3.4　扫描激光热丝焊接的间隙容忍度

为了降低激光填丝焊接技术对工件装夹精度的要求，本文还研究了不同参数下激光填丝焊的对接间隙容忍度，实验结果如图 12、13 所示。在研究对接间隙的工艺实验中，固定激光功率 P=1.8 kW，焊接速度 V_w=1.0 m/min，送丝速度 V_f=3.0 m/min。从图 12 可以看出，在保证焊缝成形良好、无塌陷的情况下，对于 2 mm 厚的 Q235 钢，激光冷丝焊接所允许的最大对接间隙为 1 mm，当间隙提高到 1.1 mm 时，如图 13(a)、(b)所示，由于聚焦光斑很小，激光能量从间隙中漏出，故焊缝产生严重的咬边和侧壁未熔合现象。加入 I=100 A 的热丝电流后，最大对接间隙提高至 1.1 mm，提升了 10%。当间隙为 1.2 mm 时，如图 13(c)、(d)所示，激光热丝焊接焊缝也出现了明显的侧壁未熔合现象，熔化区金属基本只附着在焊缝一侧。加入 A=1 mm、f=50 Hz 的扫描激光束后，当间隙为 1.3 mm 时仍能得到无缺陷、成形良好的焊缝，当间隙为 1.4 mm 时焊缝出现了塌陷。相比激光热丝焊接，扫描激光热丝焊接将最大对接间隙提升了约 18.2%，达到了母材板厚的 65%。这是因为焊缝侧壁熔化的热量主要来自热传导[25]，扫描激光热丝焊接通过扩大激光作用范围，提高了远离焊缝中心线两侧的熔池温度，并且扫描激光产生的涡流将熔池中心的高温液态金属带向侧壁，进一步促进了基板侧壁的熔化，在液桥作用下[26]，母材侧壁对熔池内熔融金属的吸附力增大，从而避免了咬边、侧壁未熔合等焊缝缺陷的产生，提高了激光热丝焊接的间隙容忍度。

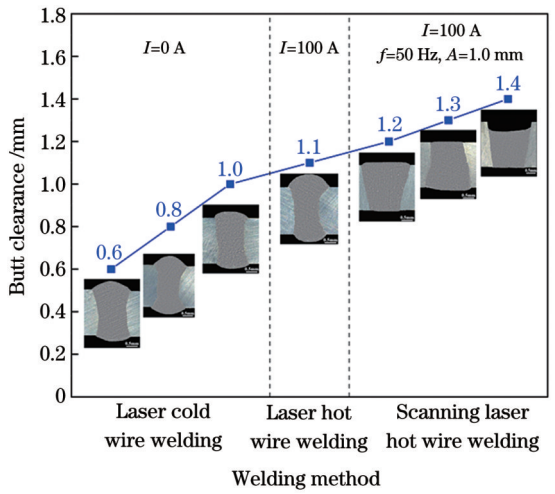

图 12　不同对接间隙下的焊缝截面形貌

Fig. 12　Appearances of weld sections under different butt clearances

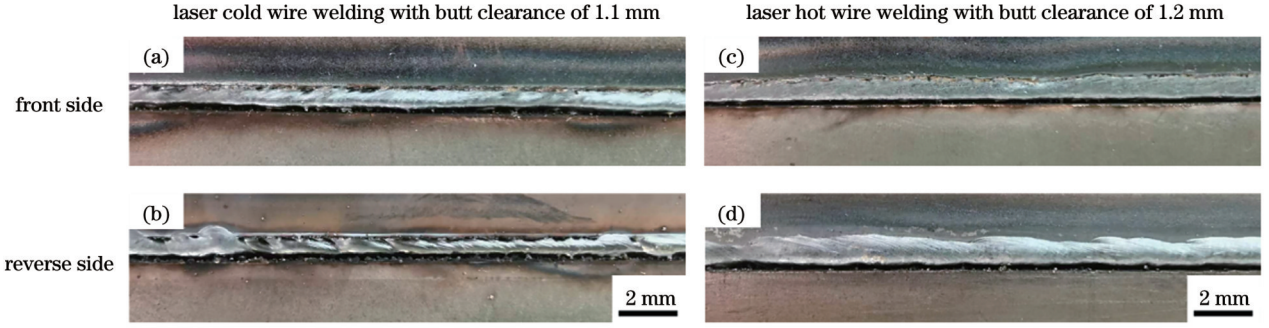

图 13　焊缝形貌

Fig. 13　Weld morphologies

4　结　　论

在扫描激光热丝焊接实验中优化了工艺参数，当扫描直径为 0.4～1.0 mm、扫描频率为 50～200 Hz 时，所得到的焊缝均成形良好，焊缝平整无缺陷，且几乎无飞溅，证明了扫描激光对焊缝成形具有良好的改善作用。同时，扫描激光提高了激光热丝焊接的间隙容忍度，有利于在间隙不均匀时实现稳定焊接，得到与母材侧壁熔合良好、表面无塌陷的焊缝。扫描激光对焊接熔池的搅拌作用能够促进熔池流动，细化晶粒，扫描激光热丝焊接焊缝熔合区组织主要为细晶铁素体和针状铁素体。相比之下，激光热丝焊接焊缝熔合区组织主要为较粗大的板条铁素体。

相比激光热丝焊接，扫描激光热丝焊接接头在抗拉强度基本不变的情况下，断口延伸率提升至 13.1%，说明加入扫描激光可有效提高焊缝的韧性，断口电镜图中更深的韧窝也证明了这一点。

激光热丝焊接焊缝熔合区的硬度最高，热影响区其次，母材硬度最低。扫描激光热丝焊接焊缝的熔合区硬度低于激光热丝焊接，这主要是因为激光热丝焊接焊缝熔合区易发生偏析，生成的夹杂物提高了显微硬度。

参　考　文　献

[1]　金周明，黄浩远，赵越．激光焊接技术在微电子行业的应用[J].

电子元器件与信息技术, 2021, 5(4): 21-22.
Jin Z M, Huang H Y, Zhao Y. Application of laser welding technology in microelectronics industry[J]. Electronic Components and Information Technology, 2021, 5(4): 21-22.

[2] 熊保胜. 汽车制造中激光焊接技术的有效应用[J]. 现代工业经济和信息化, 2022, 12(9): 218-219, 256.
Xiong B S. Effective application of laser welding technology in automobile manufacturing[J]. Modern Industrial Economy and Informationization, 2022, 12(9): 218-219, 256.

[3] 陆建卫. 激光焊接技术的研究现状及应用[J]. 科技资讯, 2021, 19(25): 41-43.
Lu J W. Research status and application of laser welding technology [J]. Science & Technology Information, 2021, 19(25): 41-43.

[4] 石秋红. 基于激光技术的船用钢板焊接性能分析[J]. 舰船科学技术, 2021, 43(16): 190-192.
Shi Q H. Welding performance analysis of marine steel plate based on laser technology[J]. Ship Science and Technology, 2021, 43 (16): 190-192.

[5] 余阳春. 激光填丝焊的焊丝熔入行为及工艺研究[D]. 武汉: 华中科技大学, 2010.
Yu Y C. Study on welding wire penetration behavior and technology of laser wire filling welding[D]. Wuhan: Huazhong University of Science and Technology, 2010.

[6] Li S C, Xu W, Xiao G, et al. Effects of Sc on laser hot-wire welding performance of 7075 aluminum alloy[J]. Materials Research Express, 2020, 7(10): 106506.

[7] 方乃文, 黄瑞生, 龙伟民, 等. 填充金属对TC4钛合金激光填丝焊接头组织性能影响[J]. 稀有金属材料与工程, 2023, 52(5): 1725-1736.
Fang N W, Huang R S, Long W M, et al. Effect of filler metal on microstructure and properties of titanium alloy laser welding joints with filler wire[J]. Rare Metal Materials and Engineering, 2023, 52 (5): 1725-1736.

[8] Shi G, Hilton P. A comparison of the gap bridging capability of CO_2 laser and hybrid CO_2 laser MAG welding on 8 mm thickness C-MN steel plate[C]//58th Annual Assembly and International Conference of International Institute of Welding, July 14-15, 2005, Prague, Czech Republic. [S.l.: s.n.], 2005.

[9] 郑世卿, 温鹏, 单际国. 激光热丝焊焊缝熔合比和焊缝深度方向的微观成分均匀性[J]. 焊接学报, 2012, 33(12): 45-48, 72, 115.
Zheng S Q, Wen P, Shan J G. Experimental analysis on fusion ratio and composition uniformity of laser hot wire welds[J]. Transactions of the China Welding Institution, 2012, 33(12): 45-48, 72, 115.

[10] Marumoto K, Tamata H, Fujinaga A, et al. Bead shape control in high-speed fillet welding using hot-wire GMA laser hybrid welding technology[J]. Welding in the World, 2023, 67(5): 1259-1266.

[11] Wei S P, Wang G, Shin Y C, et al. Comprehensive modeling of transport phenomena in laser hot-wire deposition process[J]. International Journal of Heat and Mass Transfer, 2018, 125: 1356-1368.

[12] Liu W, Ma J J, Liu S, et al. Experimental and numerical investigation of laser hot wire welding[J]. The International Journal of Advanced Manufacturing Technology, 2015, 78(9): 1485-1499.

[13] 郑世卿, 温鹏, 单际国. 激光热丝焊接过程焊丝过渡行为及其稳定性的研究[J]. 中国激光, 2014, 41(4): 0403008.
Zheng S Q, Wen P, Shan J G. Research on wire transfer and its stability in laser hot wire welding process[J]. Chinese Journal of Lasers, 2014, 41(4): 0403008.

[14] 王孝虎. 铝合金激光填丝焊缺陷分析及改进措施研究[D]. 哈尔滨: 哈尔滨工业大学, 2015.
Wang X H. Defect analysis and improvement measures of aluminum alloy laser wire filler welding[D]. Harbin: Harbin Institute of Technology, 2015.

[15] Haubold M W, Zäh M F. Real-time spatter detection in laser welding with beam oscillation[J]. Procedia CIRP, 2019, 79: 159-164.

[16] Wu M P, Luo Z, Li Y, et al. Effect of oscillation modes on weld formation and pores of laser welding in the horizontal position[J]. Optics & Laser Technology, 2023, 158: 108801.

[17] 陈根余, 王彬, 钟沛新, 等. 2060铝锂合金扫描填丝焊接工艺[J]. 焊接学报, 2020, 41(4): 44-50, 99.
Chen G Y, Wang B, Zhong P X, et al. Laser scanning welding of 2060 Al-Li alloy with filler wire[J]. Transactions of the China Welding Institution, 2020, 41(4): 44-50, 99.

[18] Li J Z, Sun Q J, Kang K X, et al. Process stability and parameters optimization of narrow-gap laser vertical welding with hot wire for thick stainless steel in nuclear power plant[J]. Optics & Laser Technology, 2020, 123: 105921.

[19] 彭进, 王星星, 李刚, 等. 激光填丝焊对熔池动态行为及焊缝成形的影响[J]. 中国激光, 2017, 44(11): 1102004.
Peng J, Wang X X, Li G, et al. Effect of laser welding with filler wire on molten pool dynamic behavior and weld formation[J]. Chinese Journal of Lasers, 2017, 44(11): 1102004.

[20] 刘招, 潘丽华, 李晓强, 等. 基于熔透模式的30Cr3超高强钢激光焊接头组织和性能研究[J]. 中国激光, 2023, 50(12): 1202104.
Liu Z, Pan L H, Li X Q, et al. Study on microstructure and properties of laser-welded 30Cr3 ultra-high-strength steel joints based on weld penetration mode[J]. Chinese Journal of Lasers, 2023, 50(12): 1202104.

[21] Shi L, Jiang L, Gao M. Numerical research on melt pool dynamics of oscillating laser-arc hybrid welding[J]. International Journal of Heat and Mass Transfer, 2022, 185: 122421.

[22] 张文钺. 焊接冶金学: 基本原理[M]. 北京: 机械工业出版社, 2002.
Zhang W Y. Welding metallurgy: basic principles[M]. Beijing: China Machine Press, 2002.

[23] 王磊. 高强铝合金振荡扫描激光束-电弧复合焊接工艺与机理研究[D]. 武汉: 华中科技大学, 2018.
Wang L. Study on technology and mechanism of oscillating scanning laser beam-arc hybrid welding of high strength aluminum alloy[D]. Wuhan: Huazhong University of Science and Technology, 2018.

[24] KouSindo. 焊接冶金学[M]. 闫久春, 杨建国, 张广军, 译. 北京: 高等教育出版社, 2012.
Koua S. Welding metallurgy[M]. Yan J C, Yang J G, Zhang G J, Transl. Beijing: Higher Education Press, 2012.

[25] Ma C Y, Chen B, Meng Z, et al. Characteristic of keyhole, molten pool and microstructure of oscillating laser TIG hybrid welding[J]. Optics & Laser Technology, 2023, 161: 109142.

[26] 项云忠. 6061/2A12异种铝合金激光扫描焊接接头组织性能研究[D]. 武汉: 华中科技大学, 2019.
Xiang Y Z. Study on microstructure and properties of laser scanning welded joint of 6061/2A12 heterogeneous aluminum alloy [D]. Wuhan: Huazhong University of Science and Technology, 2019.

Process Characteristics, Microstructure, and Properties of Q235 Steel by Scanning Laser Hot Wire Welding

Yu Chenqian[1], Ren Gang[2], Huang Yingjie[2], Gao Ming[1*]

[1]*Wuhan National Laboratory for Optoelectronics, Huazhong University of Science and Technology, Wuhan* 430074, *Hubei, China*;

[2]*Jiujiang Institute of Advanced Laser Technology, Jiujiang* 332005, *Jiangxi, China*

Abstract

Objective Laser welding has the characteristics of a high energy density, low heat input, and high welding efficiency; however, conventional laser welding has a small focused spot and high requirements for the welding assembly gap. To solve this problem, scholars have developed laser wire filling welding technology. Based on this, some scholars have developed laser hot wire welding technology, which can effectively improve the absorptivity of the welding wire by preheating the welding wire in advance, reduce the requirements for laser power, and improve the welding speed; however, there are still problems such as high requirements for the alignment of the laser focus and the tip of the welding wire, and an uneven weld height. In this study, the process characteristics of Q235 steel by scanning laser hot wire welding are systematically studied, and the mechanism of the influence of the scanning laser on the solidification process of weld metal is clarified, which provides technical guidance for expanding the industrial application of laser welding.

Methods The base material used in this study is the Q235 steel plate. The size is 50 mm×120 mm×2 mm, and the structure is massive ferrite at normal temperature. The flat surfacing welding method is used in the research on the weld surface and section forming. The docking method is adopted in the study of the microstructure and properties of welded joints. According to the previous research and accumulation of this research group, the fixed wire feeding method is front wire feeding, the tilt angle of the welding torch is 45°, and the laser focus is located on the surface of the plate, that is, the defocus quantity is 0 mm. In the welding process, the shielding gas is argon with purity (volume fraction) greater than 99.99%. The gas pipe angle is 60° and the gas flow rate is approximately 20 L/min. In the butt welding experiment, the fixed laser power is 1.8 kW, the welding speed is 1.0 m/min, the preheating current of laser cold wire welding is 0 A, the preheating current of laser hot wire welding is 100 A, the scanning amplitude ranges from 0.6 mm to 1.0 mm, and the scanning frequency ranges from 100 Hz to 200 Hz.

Results and Discussions Under different scanning parameters, the distribution of the laser energy is different, which affects the temperature field distribution of the weld pool, and then affects the macro forming, microstructure, and properties of the weld. Compared with that in non-scanning laser hot wire welding, the weld forming in scanning laser hot wire welding is smoother and straighter, and the splash is less (Fig. 5). The weld structure in non-scanning laser hot wire welding is dominated by thick side lath ferrite. Because the scanning laser enhances the flow of the molten pool through the stirring effect and breaks the coarse columnar crystals, the weld structure in scanning laser hot wire welding is dominated by fine crystalline ferrite and acicular ferrite with finer grains (Fig. 7). The tensile strength (578.8 MPa) of the scanning laser hot wire welded joint is basically the same as that (574.7 MPa) of the non- scanning laser hot wire welded joint, but the elongation is increased from 8.4% to 13.1% (Table 3). The dimple size of the tensile fracture surface of the scanning laser hot wire welded joint is more uniform, and the dimple size difference between the laser hot wire welded joint and the laser cold wire welded joint is larger; moreover, there is obvious inclusion precipitation at the bottom of the dimple, indicating that the scanning laser improves the homogeneity of the weld structure (Fig. 10). Simultaneously, the scanning laser improves the gap tolerance during butt welding. In the butt welding experiment of the Q235 steel plate with a thickness of 2 mm, the scanning laser hot wire welding ensures good weld formation without defects when the gap is 1.3 mm (Fig. 12).

Conclusions In the experiment of scanning laser hot wire welding, by optimizing the process parameters, when the scanning diameter is 0.4–1.0 mm and the scanning frequency is 50–200 Hz, the welds obtained are well formed, smooth, no defects and nearly no splash, which proves that the scanning laser has a good improvement effect on the weld formation. Simultaneously, the scanning laser improves the gap tolerance of laser hot wire welding, which is conducive to achieve stable welding when the gap is uneven and obtain a weld with good fusion with the base metal side wall and no surface collapse. At the microstructure level, the stirring effect of the scanning laser on the weld pool can promote the flow of the weld pool and refine the grain. In terms of mechanical properties, compared with that in non- scanning laser hot wire welding, when the tensile strength is basically unchanged, the fracture elongation increases to 13.1% in scanning laser hot wire welding, indicating that the addition of the scanning laser can effectively improve the toughness of the weld, which is also proved by the deeper dimples in the electron microscope image of the fracture. The hardness of the fusion zone in the laser hot wire welding is the highest, followed by that of the heat affected zone, whereas the hardness of the base metal is the lowest. The hardness of the fusion zone in the scanning laser hot wire welding is lower than that in the non- scanning laser hot wire welding, mainly because the fusion zone in the non- scanning laser hot wire welding is easy to produce segregation, and the generated inclusions increase the microhardness.

Key words laser technique; laser hot wire welding; laser beam scanning; microstructure; mechanical properties